Network Performance Enhancement by Implementing Self-Healing functions in Mobile Network Operations

M. Cilínio
Instituto Superior Técnico
madalena.ramos@tecnico.ulisboa.pt

***Abstract*—Detecting and diagnosing the root cause of failures in mobile networks is an increasingly demanding and time-consuming task, given its technological growing complexity. This work focuses on performing the Root Cause Analysis (RCA) of mobile network Key Performance Indicators (KPIs) failures, using supervised learning and the Tree Shapley Additive Explanations (SHAP) method. To fulfill this objective, ensemble classification models are used to predict a failure/non-failure binary label. The influence of each counter on the overall model's predictive performance is performed based on the TreeSHAP method. The described methodology allows to successfully predict failures in the User Downlink (DL) Average Throughput, User Uplink (UL) Average Throughput and Service Drop Rate KPIs. Moreover, not only the most critical counters for fault detection and diagnosis are identified, as the respective influence is analyzed in detail. Lastly, based on the identification of the most critical PM counters, it is not only possible to identify and quantify the KPIs failures, but also to outline a process for solving them.**

***Index Terms*—Mobile Networks, LTE, KPIs, Counters, RCA, Machine Learning, TreeSHAP**

I. Introduction

The exponential complexity growth of mobile networks has brought challenges in performing the RCA of network performance degradation resorting only to human input. For this reason, Mobile Network Operators (MNOs) have turned their attention to automating this analysis by introducing Self-Healing functions divided into three primary areas: Detection, Diagnosis and Compensation [1] . The main target of these Self-Healing functions is to automate troubleshooting tasks by minimizing the occurrence of partial and full outages, as well as their manual detection and compensation. These functions are based on correlation and statistical analysis of several sources of data, which may include: alarms, mobile traces, configuration parameters, network counters and KPIs [2]. Thus, Machine Learning (ML) techniques have emerged as a powerful tool to develop Self-Healing networks, due to their ability to learn from the available data to effectively reproduce the decisions made by human experts.

The main objective of this work is to determine the root cause of KPIs performance degradation using Performance Management (PM) counters as input features to supervised learning algorithms. Thus, classification models are used to predict a failure/non-failure binary label. The respective RCA is performed based on SHAP method, which provides a more interpretive analysis for each model output. In this context, the main contributions of this work can be summarized as follows: i) Implementation of a network failure's diagnostic system based on PM counters measured from a real mobile network and ii) Introduction of a feature filtering method that speeds up the diagnosis process by reducing the total number of influential PM counters to be analysed by network engineers.

This work is organized as follows: Section II summarizes the research methodology; Section III presents the obtained results for the failure prediction models and the respective SHAP method applied to the selected KPIs; Section IV analyzes the output of the SHAP method in order to perform the RCA of the predicted failures. Ultimately, Section V presents the final conclusions and research guidelines for future work.

II. Methodology

The PM counters used in the elaboration of this work were obtained from a real MNO, having been collected from a live Long Term Evolution (LTE) network. The data extraction was performed with an hourly granularity, over a period of 28 days, from 19 sites supporting the LTE800, LTE900, LTE1800 and LTE2100 (MHz) frequency bands. The resulting dataset comprises a total of 337 PM counters referring to the six categories of network performance indicators specified by the 3rd Generation Partnership Project (3GPP): Accessibility, Retainability, Availability, Integrity, Mobility and Utilization.

A. KPIs Computation

Through the combination of the 337 collected PM counters, 13 KPIs were calculated. However, no Mobility KPI has been used since LTE technology already exploits the Automatic Neighbor Relations (ANR) and Mobility Robustness Optimization (MRO) solutions. While the ANR is responsible for reducing the human interaction in the process of managing neighbor cells relations, the MRO identifies the root cause of Mobility KPIs degradation, in order to automatically adjust the mobility parameters for the optimal configuration [3]. Thus, both ANR and MRO are Self-Organizing Network (SON) mechanisms that already improve the performance of the Mobility KPIs, as intended with this work.

B. Data Pre-Processing and Feature Selection

Since the data was collected from a live network, being subject to extraction failures, it was necessary to perform some data pre-processing and feature selection processes first. Both processes encompassed data cleaning steps such as eliminating null values, data artifacts and features with null variance.

C. Labelling

The failures detection techniques using classification models imply the existence of a discrete dependent variable. Thereby, a binary faulty/not faulty label was defined by applying degradation threshold values to the KPI to be predicted. These threshold values were provided by the MNO. Therefore, while *label 1* was assigned to failures, *label 0* was assigned to not faulty samples. After defining the dependent discrete variable for each KPI, the counters used in its calculation, as well as counters redundant to these, were eliminated from the feature set to avoid the occurrence of overfitting.

D. Machine Learning Techniques

Although ML classification algorithms are a powerful tool in detecting network failures, there are still challenges related to their implementation that need to be considered [4]:

- **Cost Insensitivity**: Different misclassification errors may have different impact on mobile operators, being essential to assign variable costs to different errors.
- **Data Imbalance**: Since cellular network's severe degradation are infrequent events, the collected training data tend to be significantly imbalanced. As a result, the minority class tends to be misclassified more often than the majority class.

Thereby, the ML classification models implemented and tested throughout this work were the following: AdaBoost, Gradient Boosting, XGBoost, Random Forest and ExtraTrees. Regarding the performance evaluation metric it was required to choose a technique that took into account the non-balancing between classes. To address this issue, the F1-score function was selected, as suggested by [5]. This function is given by the harmonic mean of precision and recall, reaching its best value at 1 and worst score at 0 [6].

Lastly, the Stratified 10-Fold Cross-Validation technique was implemented, in order to evaluate the model's generalization performance, by detecting overfitted models. This technique has the particularity of ensuring that when splitting the dataset, the class distribution in each subset matches the class distribution in the total training set, avoiding the existence of folds with few or no data belonging to the minority class

E. Shapley Additive Explanations

In this phase, the SHAP method is applied to interpret the outputs of the selected models by computing the contribution of each input feature in the produced predictions [7] [8]. This method calculates the Shapley values, given by the average of all features contributions, considering all possible coalitions. These Shapley values are represented as an additive feature attribution method. In this work, it was used a variant of SHAP for tree-based ML models, designated TreeSHAP.

III. Failures Detection

From the 337 PM counters provided by the MNO, the following KPIs were calculated: Radio Resource Control (RRC) Setup Success Rate (%), RRC Setup Success Rate (Signaling) (%), E-UTRAN Radio Access Bearer (E-RAB) Setup Success Rate (%), Call Setup Sucess Rate (%), User DL Average Throughput (Mbps), User UL Average Throughput (Mbps), DL Packet Loss Rate (%), UL Packet Loss Rate (%) and Service Drop Rate (%) [9]. After proceeding with the data pre-processing and feature selection phases, the number of input features was reduced to 223 PM counters. Hereupon, the binary failure labelling process and the ML classification models mentioned in Section II were implemented. Table I summarizes the obtained results for the best performing classification model applied to each KPI.

TABLE I
Results obtained for the ML models.

KPI	Failure Threshold	Binary Labelling	Model	F1 Score	10-Fold Cross Validation
RRC Setup Success Rate	$< 98\%$	0 : 34130 samples 1 : 94 samples	Gradient Boosting	0.129	-
RRC Setup Success Rate (Signaling)	$< 98\%$	0 : 33901 samples 1 : 371 samples	XGBoost	0.152	-
E-RAB Setup Success Rate	$< 98\%$	0 : 33971 samples 1 : 253 samples	XGBoost	0.203	-
Call Setup Success Rate	$< 98\%$	0 : 33765 samples 1 : 459 samples	XGBoost	0.139	-
User Downlink Average Throughput	< 7 Mbps	0 : 26789 samples 1 : 7482 samples	XGBoost	0.867	0.849
User Uplink Average Throughput	< 0.5 Mbps	0 : 30681 samples 1 : 3543 samples	XGBoost	0.716	0.704
Downlink Packet Loss Rate	$> 2\%$	0 : 34192 samples 1 : 32 samples	XGBoost	0.600	0.400
Uplink Packet Loss Rate	$> 2\%$	0 : 34051 samples 1 : 173 samples	XGBoost	0.302	-
Service Drop Rate	$> 2\%$	0 : 33553 samples 1 : 671 samples	XGBoost	0.586	0.584

The RRC Setup Success Rate, RRC Setup Success Rate (Signaling), E-RAB Setup Success Rate and Call Setup Success Rate, categorized into Accessibility KPIs, and the UL Packet Loss Rate, categorized into Integrity KPI, presented the lowest failure prediction performances. As a result, these KPIs were immediately excluded from the RCA phase. In contrast, the prediction of failures in the DL Packet Loss Rate, categorized into Integrity KPI, and in the Service Drop Rate, categorized into Retainability KPI, was performed with greater success. However, it is possible to verify the occurrence of overfitting in the model that predicts failures in the DL Packet Loss Rate KPI. This situation is identified by the marked decrease in the model's performance when applying the Stratified 10-fold cross-validation technique. In this way, only the Service Drop Rate KPI advanced to the RCA phase. Lastly, the User UL Average Throughput and the User DL Average Throughput, both categorized into Integrity KPIs, presented F1-scores which reveal a great ability of the models

to predict network degradation. Thus, both KPIs proceeded to the RCA phase.

Thereby, the TreeSHAP method was implemented to the three selected KPIs. This SHAP method variant was used since the decision-tree-based ensemble XGBoost algorithm was the best performing model for all the selected KPIs. At this stage, the most important features for the models prediction were filtered using the top 85th percentile of the best mean absolute value for the SHAP values. The detailed analysis of the obtained results is provided below.

A. User DL Average Throughput

Regarding the User DL Average Throughput KPI, the best performing model presented a F1-score of 0.867. Table II illustrates the obtained confusion matrix.

TABLE II
CONFUSION MATRIX OBTAINED FOR USER DL AVERAGE THROUGHPUT.

		Predicted Label	
		0 (Non Failure)	1 (Failure)
True Label	0 (Non Failure)	6424	255
	1 (Failure)	250	1639

In turn, Fig. 1 illustrates the Summary Plot, which provides a high-level analysis for each feature importance, sorted in descending order.

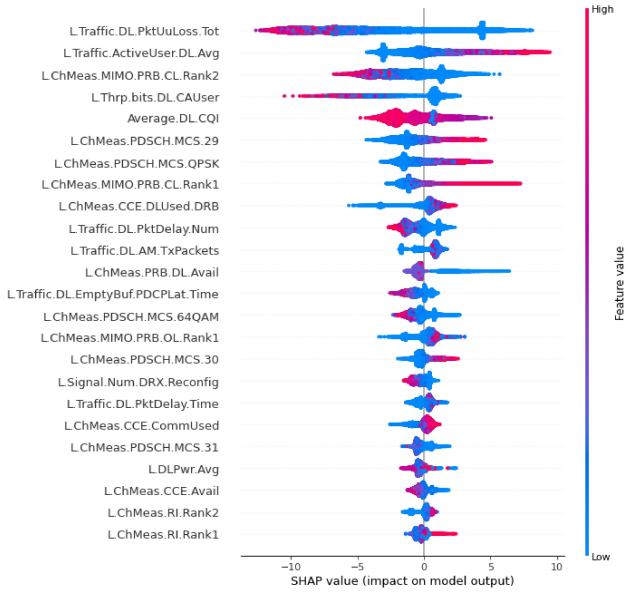

Fig. 1. SHAP Summary Plot for User DL Average Throughput failure prediction.

While the x-axis represents the Shapley values, in which the positive values are indicative of *label 1* and the negative values of *label 0*, the y-axis represents each feature. In turn, the color illustrates the feature's values, with the highest ones being represented in pink and the lowest ones in blue. For example, analyzing the L.ChMeas.CCE.DLUsed.DRB counter, it is verified that higher values of this feature contribute to the attribution of *label 1*. That is, the pink samples of this feature are mostly on the positive x-axis. On the other hand, lower values contribute to the attribution of *label 0*, since the blue samples are mostly distributed in the negative x-axis. This happens since the Physical Downlink Control Channel (PDCCH) uses aggregation layers in groups of 1, 2, 4 or 8 Control Channel Elements (CCEs), based on radio conditions. Thus, while a User Equipment (UE) in good radio condition requires only 1 CCE, a UE in poor radio coverage may require 8 CCEs to provide greater decoding redundancy [10].

B. User UL Average Throughput

Regarding the User UL Average Throughput KPI, the best performing model presented a F1-score of 0.716. While Table III illustrates the obtained confusion matrix, Fig. 2 represents the respective SHAP Summary Plot.

TABLE III
CONFUSION MATRIX OBTAINED FOR USER UL AVERAGE THROUGHPUT.

		Predicted Label	
		0 (Non Failure)	1 (Failure)
True Label	0 (Non Failure)	7389	229
	1 (Failure)	293	657

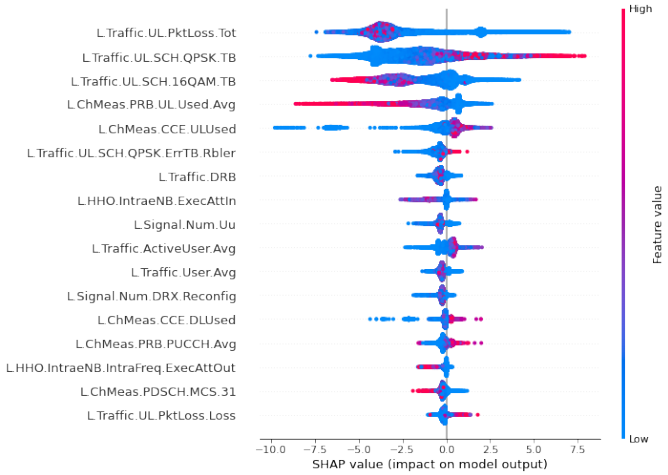

Fig. 2. SHAP Summary Plot for User UL Average Throughput failure prediction.

C. Service Drop Rate

Lastly, regarding the Service Drop Rate KPI, the best performing model presented a F1-score of 0.586. Table IV represents the obtained confusion matrix and Fig. 3 illustrates the respective SHAP Summary Plot.

TABLE IV
CONFUSION MATRIX OBTAINED FOR SERVICE DROP RATE.

		Predicted Label	
		0 (Non Failure)	1 (Failure)
True Label	0 (Non Failure)	8375	86
	1 (Failure)	20	75

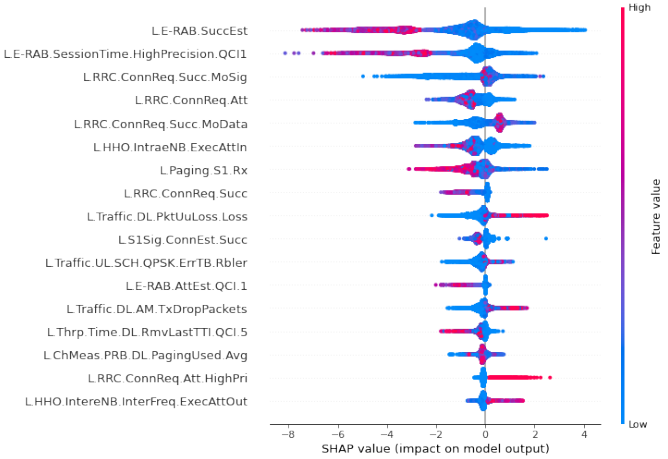

Fig. 3. SHAP Summary Plot for Service Drop Rate failure prediction.

The detailed analysis of the obtained results is provided in the next section, presenting the RCA of the model's failures predictions.

IV. ROOT CAUSE ANALYSIS

A. User DL Average Throughput

Diagnosing the causes of low throughput is a complex process that requires in-depth knowledge of the network operation, being often a time-consuming task for the network engineers. Thus, the following analysis aims to identify the three main causes of throughput degradation, listed in Table V, from the analysis of the obtained SHAP Summary Plot.

TABLE V
MAIN CAUSES FOR THROUGHPUT DEGRADATION.

Failures	Typical causes
Configuration problems	Misadjusted configuration parameters
Radio link problems	Lack of coverage or high interference
Capacity problems	Low capacity in traffic and control channels

The User DL Average Throughput specifies the average DL throughput assigned to each UE in a cell. Thereby, increasing the L.Traffic.ActiveUser.DL.Avg counter, given by the average number of activated UEs in DL, leads to a decrease in the DL throughput, since the resource usage is shared within the available bandwidth, as illustrated by the SHAP dependence plot of Fig. 4.

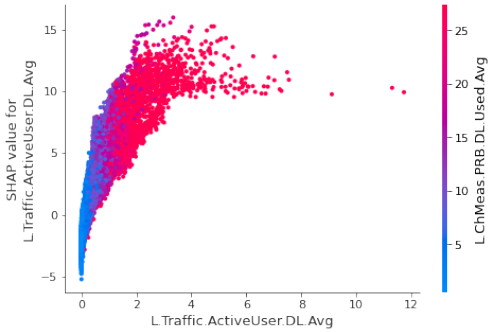

Fig. 4. SHAP dependence plot between the L.Traffic.ActiveUser.DL.Avg and L.ChMeas.PRB.DL.Used.Avg counters.

Thus, Fig. 4 shows that when the average number of activated UEs in DL increases, the L.ChMeas.PRB.DL.Used.Avg counter, given by the average number of used Physical Downlink Shared Channel (PDSCH) Physical Resource Blocks (PRBs) in DL, also increases, contributing to User DL Average Throughput degradation, since these points are mostly distributed on the positive SHAP values axis. In this situation, so that each user's experience is not affected, it may be necessary to increase the Inactivity Timer, which controls the transition from RRC_CONNECTED to RRC_IDLE state. Thereby, an UE is connected if it has at least one established Dedicated Radio Bearer (DRB). Once there is no more traffic in the transmit buffer, the UE continues in the RRC_CONNECTED state for a defined period of time. If during this period of time it does not detect any traffic, the UE switches to the RRC_IDLE state. Thus, by decreasing the value of the Inactivity Timer parameter, it is possible to support more UEs in the connected state, which can lead to network congestion. On the other hand, by increasing the value of this parameter, it is possible to improve the overall throughput for each UE. However, if this parameter assumes very high values, it is also possible that some UEs use more resources than necessary. Thus, this parameter must be optimized by balancing these two situations. Therefore, engineers' first approach for solving low throughput problems caused by a high number of users should be to adjust the Inactivity Timer configuration parameter. Another solution to reduce the high PRB utilization, caused by the increased number of UEs in a cell, is to distribute the traffic by less used neighboring cells. Still regarding Fig. 4, it is possible to verify the existence of some pink dots, that is, a high average number of used PDSCH PRBs, for low L.Traffic.ActiveUser.DL.Avg values, corresponding to a degradation of the User DL Average Throughput KPI, since the respective SHAP value, represented on the y-axis, is positive. This situation corresponds to a problem of low network capacity, in which the number of available PRBs for DL is not enough to meet the throughput requirements.

Continuing to analyse Fig. 1, it is possible to verify that when the L.ChMeas.PDSCH.MCS.QPSK counter, which measures the number of times that Quadrature Phase Shift Keying (QPSK) Modulation and Coding Scheme (MCS) indexes are scheduled on the PDSCHs, increases, the model detects more

failures in User DL Average Throughput. On the other hand, when the L.ChMeas.PDSCH.MCS.64QAM counter, which measures the number of times that 64-Quadrature Amplitude Modulation (QAM) MCS indexes are scheduled on the PDSCHs, increases, the model detects fewer low throughput situations. Although most of the times, these counters indicate radio problems as the cause of severe throughput degradation, in a first analysis, the problem resolution must be initialized by trying to adjust Channel Quality Indicator (CQI) reports configuration parameters, as will be explained below. The deterioration of the channel's radio conditions, either due to lack of coverage or due to high interference, is identified by a low Signal-to-Interference-plus-Noise Ratio (SINR) value, measured by the UE. This value is converted into a lower CQI to the E-UTRAN NodeB (eNB), which results into a lower MCS index, as illustrated by the SHAP dependence plot of Fig. 5.

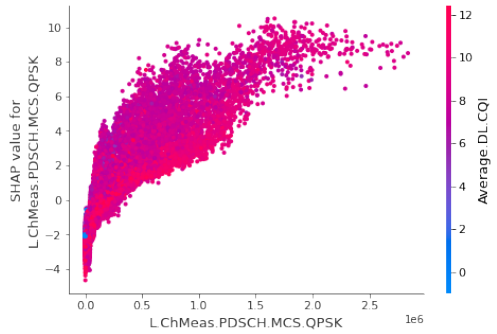

Fig. 5. SHAP dependence plot between the L.ChMeas.PDSCH.MCS.QPSK and Average.DL.CQI counters.

However, this decrease in throughput may not correspond to a permanent scenario since some vendors use conservative CQI selection algorithms. Therefore, the eNB may use a most conservative CQI value during some transmissions, while continuously monitoring the Block Error Rate (BLER) value. If after some transmissions the CQI value is maintained, the eNB converges its value to the one initially reported by the UE. The convergence of the CQI and MCS to their actual values results in increased DL throughput. Additionally, the configuration of the CQI reports periodicity must be verified, in order to ensure that it is adapted to the characteristics of each UE. If these solutions do not allow to increase the User DL Average Throughput, the next approach is to try to identify a radio link problem. In this case, some possible solutions to overcome these failures are to optimize the antennas' tilts and azimuths or increase the inter-site distance. This failure resolution strategy should also be followed for low throughput situations identified by an increased value of the L.ChMeas.PDSCH.MCS.29 counter, or a reduced value of the L.ChMeas.PDSCH.MCS.31 counter, which indicate the number of times that MCS is changed to QPSK and 64-QAM, respectively, during re-transmissions.

In turn, the L.ChMeas.MIMO.PRB.CL.Rank1 and L.ChMeas.MIMO.PRB.CL.Rank2 counters, which measure the number of used DL PRBs in closed-loop Rank 1 and 2, respectively, have a leading role in detecting throughput degradation. Namely, while an increased number of Rank 1 reports favors the detection of throughput failures, as shown in Fig. 6, an increased value of Rank 2 reports is associated with higher DL throughput values. Thereby, the Rank Indicator (RI) value gives information about the antenna layer reception, being only reported if the UE is in Multiple Input Multiple Output (MIMO) mode. While for Rank 1 a single antenna signal is transmitted using diversity, for Rank 2 spatial multiplexing is used. Thus, when the number of Rank 1 reports increases, radio engineers must first ensure that the switching system between transmission modes is correctly configured and that each UE has access to the highest possible throughput. If once again it is not possible to solve the throughput degradation by re-configuring network parameters, the radio channel degradation troubleshooting already presented should be tested.

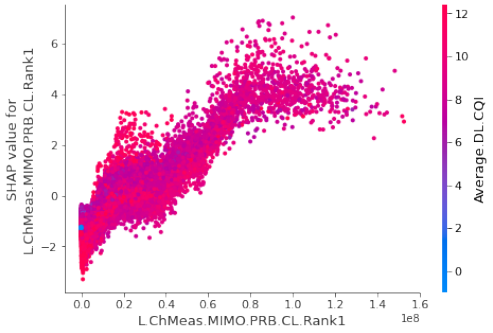

Fig. 6. SHAP dependence plot between the L.ChMeas.MIMO.PRB.CL.Rank1 and Average.DL.CQI counters.

Lastly, analysing once again Fig. 1, it is verified that the L.ChMeas.CCE.DLUsed.DRB and L.ChMeas.CCE.DLUsed counters, related with the number of used CCEs per PDCCH, are critical features for the model decision making. As explained above, a increased number of PDCCH resources usage leads to a reduced number of available resources for the PDSCH, which implies a decrease in DL throughput. In this way, these counters may alert radio engineers to situations of low DL throughput caused by radio link problems or high PDCCH capacity consumption. Thereby, a low throughput situation, in which the UEs are transmitting mostly in QPSK, with a high PDCCH capacity consumption, probably indicates a radio link problem. On the other hand, a low throughput situation, in which the UEs are mostly transmitting in 64-QAM, with a high PDCCH capacity consumption, probably indicates a network capacity problem. A possible solution that can be implemented to the last problem is the addition of new cells.

Once defined the most critical PM counters to detect failures in the User DL Average Throughput KPI, and taking into account the work developed in [11], as well as the documentation in [12], the flowchart of Fig. 7 was created to determine the most probable DL throughput degradation cause for each

site. Thus, this flowchart aims to categorize the 7482 DL throughput failures, measured in the 19 sites, in configuration, radio and capacity problems.

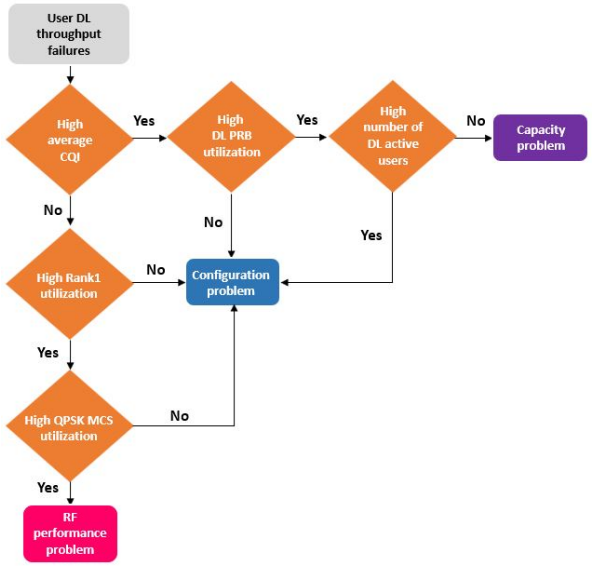

Fig. 7. RCA flowchart for User DL Average Throughput failures.

Fig. 8 not only illustrates the number of failures per site, but also their most likely causes. It was also possible to verify that failures due to misadjusted configuration are the most frequent, being responsible for 78.12% of the total problems, while radio link and capacity issues are responsible for 17.16% and 4.72%, respectively. Moreover, given the proximity of three sites with radio problems, highlighted by the purple circles in Fig. 8, it was possible to assume the existence of a high interference problem in that area. In fact, since all three sites still indicate configuration problems, possibly re-configuring the antenna tilt parameters could solve both issues.

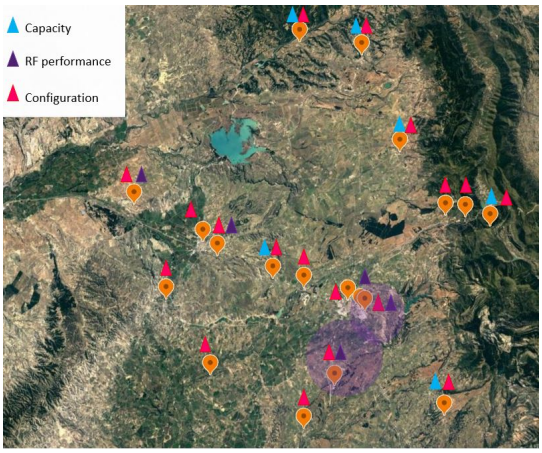

Fig. 8. Distribution of the most likely causes of DL throughput failures across the 19 sites.

In fact, while some of these problems can be solved at software level, others may involve physical changes.

B. User UL Average Throughput

Regarding the User UL Average Throughput, it is possible to verify from Fig. 2 that, similarly to what happens for the DL throughput, higher values of the L.Traffic.UL.SCH.QPSK.TB counter, given by the number of transmission blocks (TB) initially transmitted in QPSK, contributes to UL throughput degradation, while increased values of the L.Traffic.UL.SCH.16QAM.TB counter, representing the number of TBs initially transmitted in 16-QAM, leads to higher UL throughput values. Thus, to solve low UL throughput problems, identified by the growing use of robust modulation schemes, it is necessary to ensure that the UL link adaptation function, responsible for adjusting the MCS to keep the target BLER at 10%, is maximising the UL throughput. If the UL link adaptation function is working correctly, then the throughput degradation is typically caused by radio problems, as explained above.

Continuing the analysis of Fig. 2, it is verified that an increased value of the L.Traffic.UL.SCH.QPSK.ErrTB.Rbler counter, given by the total number of UL error transport blocks, after the maximum number of re-transmissions in QPSK modulation mode has been reached, favors the decrease of the User UL Average Throughput. Thus, when radio channel conditions are unfavorable, either due to high interference, or lack of coverage, data are re-transmitted with a larger number of redundant bits, in a lower modulation. However, if these data fail to be decoded after a given configurable number of re-transmissions, these data are considered residual BLER, as shown in Fig. 9. If this problem extends over time, it may be necessary for radio engineers to carry out configuration or mechanical changes to the antennas.

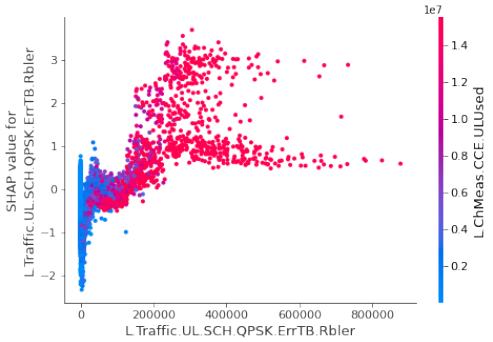

Fig. 9. SHAP dependence plot between the L.Traffic.UL.SCH.QPSK.ErrTB.Rbler and L.ChMeas.CCE.ULUsed counters.

Regarding the L.ChMeas.CCE.ULUsed counter, representing the number of PDCCH CCEs used for UL control information, it is verified that, as analysed for the DL throughput, when the value of this counter increases, the UL throughput decreases. Therefore, once more, these counters may alert radio engineers to situations of low UL throughput caused by a radio link problems or high PDCCH capacity consumption. Therefore, once more, while a high utilization of CCEs, accompanied by a high utilization of the QPSK MCS indicate

radio link problems, a high utilization of CCEs, accompanied by a low utilization of the QPSK MCS may indicate capacity problems.

It is still possible to verify that when the L.ChMeas.CCE.DLUsed counter value increases, the UL throughput decreases, and vice versa. This occurs since PDCCH carries assignments both for PDSCH, in DL, and for Physical Uplink Shared Channel (PUSCH), in UL. Thus, if a high number of PDCCH CCEs is used in the DL transmission, it may happen that the UL grant, indicating the detailed resources to be used in UL, is not scheduled in that Transmission Time Interval (TTI), for a given UE. This situation may therefore indicate a low capacity problem.

In turn, an increased value of the L.ChMeas.PRB.PUCCH.Avg counter, given by average number of used PRBs over the Physical Uplink Control Channel (PUCCH), is also associated with low UL throughput values. The PUCCH carries UL control information, taking a minimum of 2 PRBs of the UL band. These PRBs are allocated on the bandwidth extremes, in order to maximize the number of contiguous PRBs available for PUSCH allocation, which carries UL user data. Therefore, it is necessary to plan the PUCCH region, in order to have a correct balance between data and control resources. Thereby, if the number of used PRBs over the PUCCH is too high, the UL throughput decreases due to limited network capacity.

Regarding the L.ChMeas.PRB.UL.Used.Avg counter, representing the average number of used UL PRBs, it is possible to see that its increase favors the increase of the User UL Average Throughput KPI, as expected. However, it should be noted that contrary to what happens in the DL direction, an increased number of used PRBs in UL may not be always translated into greater UL throughput. Thus, if an UE is already transmitting at maximum power, an increase in the number of used PRBs will decrease the power allocated by PRB. This situation is prevented through power headroom reports, that inform the eNB of the transmission power still available in the UE. Based on this information, the eNB limits the number of scheduled PRBs, so that UL throughput is not compromised and resources are not wasted. This mechanism allows to avoid the occurrence of further degradation in the User UL Average Throughput KPI, caused by the UE's power limitation. Low power headroom reports may be generated by UL interference and maladjusted power control parameter settings. Therefore, radio engineers must be aware of these situations in order to avoid wasting network capacity.

Examining once more the SHAP Summary plot, it is verified that there are two mobility counters with great influence on the UL throughput. These counters are the L.HHO.IntraeNB.ExecAttIn, given by the number of intra-eNB incoming handover executions in a cell, and the L.HHO.IntraeNB.IntraFreq.ExecAttOut, representing the number of intra-eNB intra-frequency outgoing handovers executions in a cell. Regarding the L.HHO.IntraeNB.ExecAttIn counter, it is verified that when the number of users performing incoming handover in a sector increases, the UL throughput increases. Nevertheless, the increased number of users is not very pronounced, since these points mostly have a purple hue on the negative axis of the SHAP values. In turn, when the number of incoming handovers takes very high values, the UL throughput starts to decrease, since there may be sector congestion. This situation is described by the pink dots on the positive axis of the SHAP values. Thereby, this counter may confirm the occurrence of failures due to misconfiguration of the Inactivity Timer parameter. Regarding the L.HHO.IntraeNB.IntraFreq.ExecAttOut counter, it is verified that an increased value of the number of intra-eNB intra-frequency outgoing handovers leads to high UL throughput values, and vice-versa. This happens since the users performing outgoing handovers are at the cell boundary, with lower SINR values. Under these conditions, the users usually transmit in more robust modulation schemes, which limits the maximum data rate achieved. This is illustrated by Fig. 10, which demonstrates that as the L.HHO.IntraeNB.IntraFreq.ExecAttOut counter increases, the number of users transmitting with QPSK modulation decreases, and the UL throughput increases.

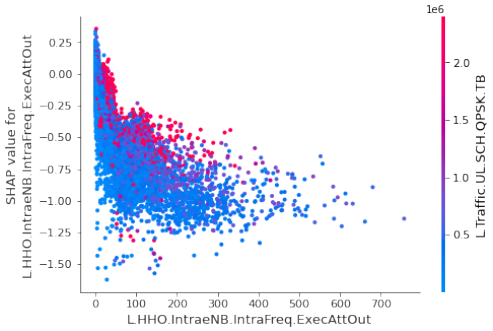

Fig. 10. SHAP dependence plot between the L.HHO.IntraeNB.IntraFreq.ExecAttOut and L.Traffic.UL.SCH.QPSK.TB counters.

Based on the identification of the most critical PM counters to detect failures in the User UL Average Throughput KPI, the flowchart of Fig. 11 was defined to categorize the 3543 total failures into configuration, radio and capacity problems. Contrary to the flowchart of the previous KPI, the number of active users in the UL was not evaluated to identify capacity problems since the associated counter was not part of dataset.

In turn, Fig. 12 illustrates the most likely failure's causes per site. It was thus verified that, similarly to what happens for the User DL Average Throughput KPI, failures due to misadjusted configuration are the most frequent, being responsible for 71.02% of the total failures, while radio link and capacity problems are responsible for 17.24% and 11.74%, respectively. Once again, given the proximity of two sites with radio problems, highlighted by the purple circles, it was possible to assume the existence of a high interference problem in that area.

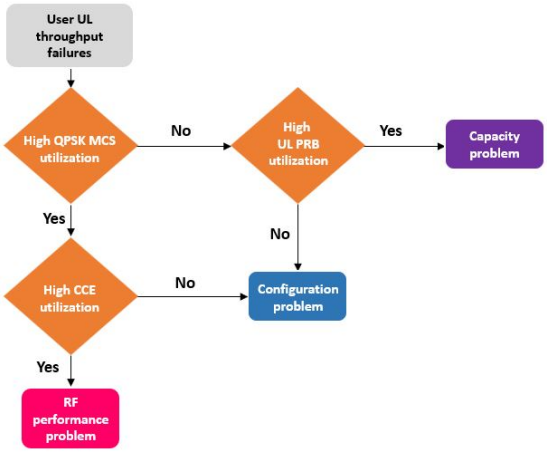

Fig. 11. RCA flowchart for User UL Average Throughput failures.

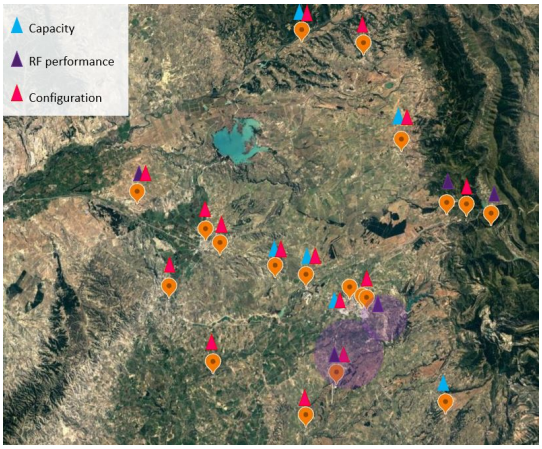

Fig. 12. Distribution of the most likely causes of UL throughput failures across the 19 sites.

C. Service Drop Rate

Lastly, the Service Drop Rate KPI specifies the service drop rate of all Quality of Service Class Identifiers (QCIs). However, contrary to what happens with the KPIs already analyzed, the causes of high Service Drop Rate are not yet so clearly defined. In this way, the root cause distinction between failures will only be presented after analyzing the respective SHAP summary plot. Thus, analysing Fig. 3, it is possible to verify that PM counters related to the number of RRC Connection Setup messages play a fundamental role in the prediction of network drop services. Namely, it is verified that low L.RRC.ConnReq.Att and L.RRC.ConnReq.Succ counters values, given by the number of RRC Connection Setup Requests excluding re-transmissions and the number of RRC Connection Setup completion times, respectively, lead to higher Service Drop Rate values. Thereby, it is necessary to identify the main causes of RRC setup failures that can lead to high network drop services. These situations can be caused by the lack of response from the UE to the RRC Connection Configuration message, or by the rejection of the eNB to the incoming RRC Connection request. The first situation can occur for a UE on the cell boundary, which sends a RRC Connection request, requiring only 7 bytes, using a small number of resource blocks with high power per carrier. However, after receiving the RRC Connection Setup message from the eNB, the UE still needs to send a RRC Connection Setup Complete message, which requires around 100 bytes. At this point, since the UE is located at the cell edge, with limited power, the average power per carrier is greatly reduced, which increases the probability of the message not being decoded by the eNB. This can also occur if the cell experiences high interference, with the eNB and UE not being able to decode the received messages. In turn, the rejection of incoming RRC Connection Requests by the eNB may be caused by resources congestion. In these situations, the eNB limits the number of new connections, since there are not enough resources to schedule new UEs. To solve these problems some solutions can be implemented. The techniques that aim to guarantee the reception of the RRC Connection Setup Complete message are to down-tilt the cell antennas, in order to remove problematic UEs, increase the timer that limits the maximum time interval between the UE sending the RRC Connection Request and receiving the RRC Connection Setup, or increase the timer that limits the maximum time interval between the eNB sending the RRC Connection Setup and receiving the RRC Connection Setup Complete message. In turn, if the problem is caused by resources congestion, a possible solution is to increase the timer value that defines the minimum time interval between RRC Connection Request messages successively sent by a given rejected UE.

Analysing Fig. 3, it is possible to verify that when the L.RRC.ConnReq.Succ.MoData counter, which measures the number of RRC Connection Setup Complete messages with a cause value of mo-Data, assumes very high values, the model detects more network drop services. This may occur due to network congestion caused by the sharp increase in the number of active users, as shown in Fig. 13.

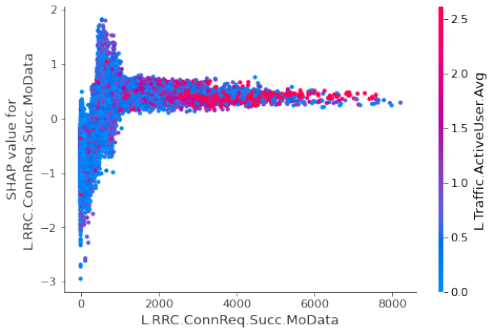

Fig. 13. SHAP dependence plot between the L.RRC.ConnReq.Succ.MoData and L.Traffic.ActiveUser.Avg counters.

In addiction, when the L.RRC.ConnReq.Att.HighPri counter value, representing the number of RRC Connection Setup attempts with a cause value of high Priority Access, increases, the Service Drop Rate also increases and vice versa. This happen since the high priority establishment cause is sent

in case the bearers are at risk of not meeting the necessary Quality of Service (QoS), thus causing service degradation.

Continuing to analyse Fig. 3, it turns out that PM counters related to the number of E-UTRAN Radio Access Bearer (E-RAB) Setups also play a crucial role in the prediction of network drop services. Namely, low values of the L.E-RAB.SuccEst, L.E-RAB.SessionTime.HighPrecision.QCI1 and L.E-RAB.AttEst.QCI.1 counters, representing the number of successful E-RAB setups initiated by UEs in a cell, the duration of data transmission for services with the QCI of 1 in a cell and the number of E-RAB setup attempts initiated by UEs for services with the QCI of 1 in a cell, respectively, contribute to high Service Drop Rate values. Thereby, by identifying the causes of failures in the establishment of E-RABs, it is possible to identify causes of high Service Drop Rate. Some possible causes are bad radio conditions, caused by high interference or weak coverage areas, intermittent S1 interface disconnections, which leads to transmission failures, and radio resources congestion, caused, for example, by a high number of active users in a cell. Some solutions to these problems have already been identified above.

From the set of features with great influence on the prediction of the Service Drop Rate KPI, the L.HHO.IntraeNB.ExecAttIn and L.HHO.IntereNB.InterFreq.ExecAttOut mobility counters also stand out. Thereby, when the L.HHO.IntraeNB.ExecAttIn counter, representing the number of intra-eNB intra-duplex-mode incoming handover executions in a cell, decreases, the Service Drop Rate increases. The opposite situation happens for the L.HHO.IntereNB.InterFreq.ExecAttOut counter, given by the number of inter-eNB inter-frequency outgoing handovers executions in a cell. This occurs since the handover procedure aims to limit the link interruption time. Thereby, for a given cell, the users perform incoming handovers if it offers better link conditions than the one to which they are connected. On the other hand, if the cell link conditions start to deteriorate, increasing the Service Drop Rate value, the users perform an outgoing handover to a cell with better radio conditions. However, the execution of handovers is not always successfully performed. Thus, a high number of handover execution failures can also lead to high service drop rate values. In these situations, the spatial arrangement of the cells must first be evaluated, in order to detect, for example, areas without coverage between the two cells, which may imply the need for physical alterations in the antennas. Other possible solutions are the reconfiguration of mobility parameters, such as updating the Neighbour Relation Table (NRT).

Lastly, examining once more the SHAP Summary plot of Fig. 3, it is verified that the L.Traffic.DL.PktUuLoss.Loss counter, given by number of DL Packet Data Convergence Protocol (PDCP) Service Data Units (SDUs) discarded for services carried on DRBs with all QCIs in a cell over the Uu interface, the L.Traffic.UL.SCH.QPSK.ErrTB.Rbler counter, representing the total number of UL error transport blocks, after the maximum number of re.transmissions in QPSK modulation mode has been reached, and the L.Traffic.DL.AM.TxDropPackets counter, given by the number of discarded DL Protocol Data Units (PDUs) in Automatic Repeat Request (ARQ) mode, have a great influence on the determination of degradation in the Service Drop Rate KPI. Namely, when the value of these counters increases, the number of network service drops also increases. Thereby, the L.Traffic.DL.PktUuLoss.Loss counter increases when the transmission delay starts to increase, which consequently leads to an increase in the Service Drop Rate KPI. In turn, the L.Traffic.UL.SCH.QPSK.ErrTB.Rbler increases when channel conditions deteriorate, which also culminates in an increase in network service drops. Finally, before analyzing the behavior of the L.Traffic.DL.AM.TxDropPackets counter, it is necessary to understand how ARQ mode works. The ARQ is an error control protocol which aims to guarantee the reliability of data transmission over an unreliable service. Thus, if the sender does not receive acknowledgment of the reception of packets, they are automatically re-transmitted. This process can be repeated a pre-defined number of times. Thereby, the L.Traffic.DL.AM.TxDropPackets counter represents the total number of discarded DL PDUs after the re-transmission limit has been reached. Thus, as the number of discarded DL PDUs increases, the Service Drop Rate also increases.

Having analyzed the most important PM counters for the model decision making, it appears that the main causes of high Service Drop Rate values are related to accessibility, mobility and traffic problems, as illustrated in Table VI.

TABLE VI
MAIN CAUSES FOR HIGH SERVICE DROP RATE VALUES.

Failures	Typical causes
Accessibility problems	RRC and E-RAB setup failures
Mobility problems	Handover execution failures
Traffic problems	Resources congestion

The flowchart of Fig. 14 was defined to categorize the 671 failures into the three main types of degradation. In turn, Fig. 15 illustrates the most likely failure's causes per site.

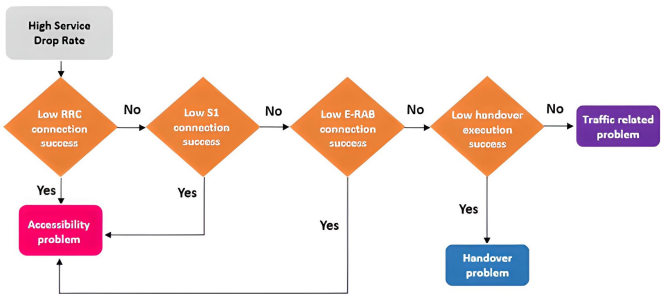

Fig. 14. RCA flowchart for Service Drop Rate failures.

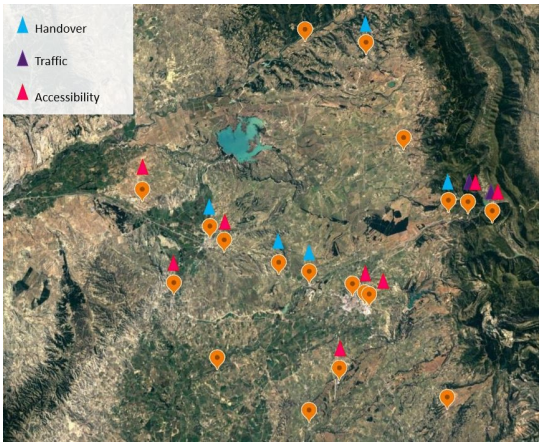

Fig. 15. Distribution of the most likely causes of Service Drop Rate failures across the 19 sites.

For this KPI, only 13 out of the 19 sites showed degraded values. It was thus verified that failures due to accessibility problems are the most frequent, being responsible for 50.60% of the total failures, while mobility and traffic problems are responsible for 19.35% and 30.05%, respectively,

Thus, it was not only possible to identify the main causes of degradation for each of the three KPIs, but also to outline some strategies for their resolution. It should be noted that although radio link and capacity problems are suggested as the source of some accessibility problems, more network data would be needed to justify these assumptions.

V. Conclusions

The main goal of this work was to determine the root cause of KPIs performance degradation using PM counters as input features to supervised learning algorithms. At the end, it should be possible to list the PM counters most likely to indicate KPI's failures symptoms, as well as define a system for diagnosing the most probable degradation cause. For this purpose, ML classification models were applied to a dataset provided by a real MNO, in order to predict a failure/non-failure binary label. The best results were obtained for the User DL Average Throughput, with a F1-score of 0.867, for the User UL Average Throughput, with a F1-score of 0.716, and for the Service Drop Rate KPI, with a F1-score of 0.586. The respective RCA, based on the TreeShap method, allowed to identify the counters that most contributed to the failures detection. Thus, counters related with the number of active UEs per cell, scheduled MCS, RI, CQI, total number of PRBs and number of CCEs per PDCCH were identified as the most important features for detecting low user throughput. Namely, it was possible to confirm that the User DL Average Throughput KPI failures were mainly distributed in configuration, radio link and capacity problems, with an incidence of 78.12%, 17.16% and 4.72%, respectively. In turn, for the User UL Average Throughput, the obtained incidence of configuration problems was 71.02%, while for radio link and capacity problems it was 17.24% and 11.74%, respectively.

Finally, the most important PM counters to indicate the root cause of high Service Drop Rate values are mainly related to accessibility, mobility and traffic issues, with an incidence of 50.60%, 19.35% and 30.05%, respectively. The identification of these features allow radio network engineers to reduce the Mean Time to Repair (MTTR), impacting not only the operational efficiency, but also the network performance.

Regarding future research, the readjustment of Configuration Management (CM) parameters, based on the failure predictions made by the models, could be tested. The ultimate goal will be to automate the adjustment of these parameters, creating cognitive Network Operations centers (NOCs) that do not require any human intervention. To achieve this goal it is necessary to complement the existing dataset, not only with new PM counters, but also with Fault Management (FM) data collected from the network. By adding more information to the dataset, it is expected to improve the predictive ability of the ML classification models. Furthermore, it would be interesting to train the models to predict network failures in advance, in order to try to mitigate their effects with early interventions. Finally, the implementation of these techniques in New Radio (NR) technology will be of utmost interest in the near future.

References

[1] A. Asghar, H. Farooq, and A. Imran, "Self-healing in emerging cellular networks: Review, challenges, and research directions,"IEEE Communications Surveys and Tutorials, vol. 20, no. 3,pp. 1682–1709, 2018.

[2] D. Mulvey, C. H. Foh, M. A. Imran, and R. Tafazolli, "Cell fault management using machine learning techniques,"IEEE Access, pp. 124514–124539, 2019.

[3] X. Zhang and X. Zhou, "Lte-advanced air interface technology", Boca Raton, London, New York: CRC Press, 2016, pp. 378–382.

[4] T. Zhang, K. Zhu, and E. Hossain, "Data-driven machine learning techniques for self-healing in cellular wireless networks: Challenges and solutions," pp. 1–7, 2019.

[5] L. A. Jeni, J. F. Cohn, and F. De La Torre, "Facing imbalanced data–recommendations for the use of performance metrics," in Affective Computing and Intelligent Interaction (ACII), 2013, pp. 245–251.

[6] F. Pedregosa, G. Varoquaux, A. Gramfort, V. Michel, B. Thirion, O. Grisel, M. Blondel, P. Pretten-hofer, R. Weiss, V. Dubourg, J. Vanderplas, A. Passos, D. Cournapeau, M. Brucher, M. Perrot, andE. Duchesnay, "Scikit-learn: Machine learning in Python,"Journal of Machine Learning Research,vol. 12, pp. 2825–2830, 2011.

[7] S. M. Lundberg and S. I. Lee, "A unified approach to interpreting model predictions,"Advancesin Neural Information Processing Systems, pp. 4766–4775, 2017.

[8] S. M. Lundberg, G. Erion, H. Chen, A. DeGrave, J. M. Prutkin, B. Nair, R. Katz, J. Himmelfarb,N. Bansal, and S.-I. Lee, "From local explanations to global understanding with explainable AI fortrees,"Nature Machine Intelligence, vol. 2, no. 1, pp. 56–67, 2020.

[9] Huawei, "KPI Reference", Int. Rep., 2014.

[10] X. Zhang, LTE Optimization Engineering Handbook, Wiley-IEEE Press, 2017.

[11] D. Parracho, D. Duarte, I. Pinto and P. Vieira, "An Improved Capacity Model based on Radio Measurements for a 4G and beyond Wireless Network", 2018 21st International Symposium on Wireless Personal Multimedia Communications (WPMC), pp. 314-318, 2018.

[12] Huawei, "eRAN Capacity Monitoring Guide", Int. Rep., 2016.